Rapid Communications

Sign switching of dimer correlations in SrCu$_2$(BO$_3$)$_2$ under hydrostatic pressure

S. Bettler ◎,* L. Stoppel ◎, Z. Yan, S. Gvasaliya, and A. Zheludev ◎†

Laboratory for Solid State Physics, ETH Zürich, 8093 Zürich, Switzerland

Magnetic and vibrational excitations in SrCu$_2$(BO$_3$)$_2$ are studied using Raman spectroscopy at hydrostatic pressures up to 34 kbar and temperatures down to 2.6 K. The frequency of a particular optical phonon, the so-called pantograph mode, shows a very strong anomalous temperature dependence below about 40 K. We link the magnitude of the effect to the magnetic exchange energy on the dimer bonds in the Sutherland-Shastry spin lattice in this material. The corresponding dimer spin correlations are quantitatively estimated and found to be strongly pressure dependent. At around $P_2 \sim 22$ kbar they switch from antiferromagnetic to being predominantly ferromagnetic.

The Shastry-Sutherland model (SSM) is arguably one of the most important constructs in the field of quantum magnetism. It demonstrates that a gapped quantum paramagnet can occur in a well-connected Heisenberg spin Hamiltonian beyond the unique topology of a single dimension. Its key feature is geometric frustration of antiferromagnetic (AF) interactions between AF $S = 1/2$ dimers arranged on a particular two-dimensional lattice [Fig. 1(a)] [1]. For sufficiently strong frustration the *exact* ground state is a product of AF singlets on each dimer bond J'. For weak frustration one recovers the semiclassical Néel-ordered phase. What happens in between has been hotly debated [2–20]. The most intriguing intermediate phase proposed is the so-called plaquette state [5,7,11]. Dimer singlets are destroyed to be replaced by singlets composed of *four* spins connected via the inter-dimer bonds J. Translational symmetry is broken and some or all of the dimer spin correlations become predominantly *ferromagnetic* (FM).

The only known and much studied experimental realization of the model is SrCu$_2$(BO$_3$)$_2$, where $S = 1/2$ Cu^{2+} ions form dimers via Cu-O-Cu superexchange pathways, which are connected through (BO$_3$) units [Fig. 1(b)] [21]. With a frustration ratio $J/J' \sim 0.6$ [22] it is reliably in the dimer phase, with a spin gap $\Delta = 3$ meV [21] in the excitation spectrum. We are incredibly lucky that in this material J/J' can be continuously tuned by hydrostatic pressure [23]. The frustration ratio increases steadily with pressure, eventually leading to a Néel-ordered state above 30 kbar [24]. Moreover, already at $P_c \sim 18$ kbar the original dimer phase gives way to a new quantum paramagnet, presumed to be the plaquette state [23–27]. Thus, theoretical predictions for exotic phases of the SSM are put to the experimental test.

How can one be sure that the novel phase is indeed plaquette rather than dimer based? To date, the only supporting evidence comes from studies of the wave-vector dependence of inelastic neutron scattering intensities [23]. Performing such measurements in a bulky cell needed to produce the required pressure for a sufficiently large sample is a formidable task. The resulting data are unavoidably limited and noisy, leaving the interpretation depending on strong assumptions and theoretical modeling [23]. In the present Rapid Communication we use an entirely different approach. We infer the strength of dimer spin correlations in SrCu$_2$(BO$_3$)$_2$ from their effect on certain optical phonons, which can be measured using Raman spectroscopy in a diamond-anvil pressure cell. We show that around P_c these correlations switch from AF to dominantly FM, and thereby independently confirm the destruction of the AF-dimer ground state. Moreover, we obtain a *quantitative* estimate for the dimer spin correlations at pressures up to 34 kbar.

The main idea is as follows. As has been established in other dimer systems, the development of pair spin correlations at low temperatures leads to a magnetic contribution to the rigidity of the corresponding bond [28–30]. This, in turn, gives rise to anomalous shifts of certain phonon frequencies at unusually low temperature. In complex structures it may be difficult to associate these shifts with any particular magnetic bonds [30]. For the highly symmetric structure of SrCu$_2$(BO$_3$)$_2$ though, the assignment of measured phonons to particular atomic motions is greatly simplified. At $\hbar\omega \sim 198$ cm^{-1} (=24.5 meV) there is a specific optical excitation, the so-called pantograph mode, visualized in Fig. 1(b) [31].

It directly modulates the intradimer coupling constant J', which is especially sensitive due to an almost 90° Cu-O-Cu [31]. At the same time, its effect on J is expected to be negligible in comparison [31,32]. The frequency of this phonon is related to the second derivative of the energy of the corresponding lattice distortion with respect to the distortion amplitude u: $\omega^2 \propto \partial^2 E / \partial u^2$. Each dimer's magnetic contribution is $J'\mathbf{S}_1\mathbf{S}_2$. The frequency of the pantograph mode is much larger than the magnetic energy scale. This ensures an adiabatic coupling scenario where the spin correlations are unaffected by the phonon which is "too fast." Since the

---

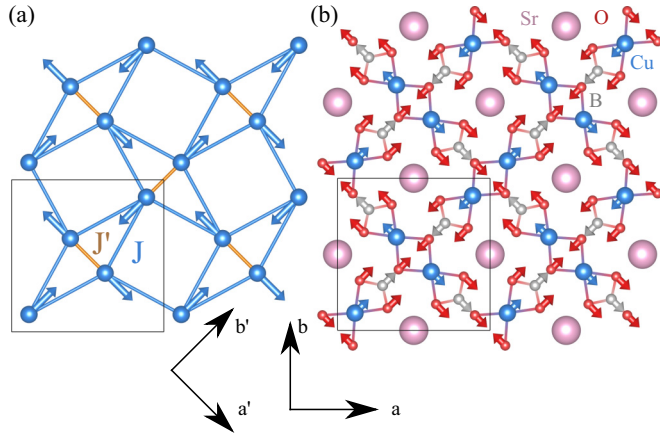*sbettler@phys.ethz.ch

†zhelud@ethz.ch; http://www.neutron.ethz.ch/

FIG. 1. (a) Lattice of orthogonal coupled dimers in $SrCu_2(BO_3)_2$ with intradimer interaction J' and interdimer interaction J. Copper atomic motions of the pantograph mode are indicated as arrows. (b) Relative atomic displacements of the pantograph mode in a single layer of $SrCu_2(BO_3)_2$.

vibration mode spans the entire sample, the magnetic energy needs to be summed (averaged) over all dimers. With this in mind,

$$\delta\omega = \omega - \omega_0 \propto \omega^2 - \omega_0^2 \propto \frac{\partial^2 J'}{\partial u^2}\langle \mathbf{S}_1\mathbf{S}_2\rangle, \tag{1}$$

where ω_0 is the mode frequency in the absence of any magnetic correlations and it is assumed that $|\omega - \omega_0| \ll \omega_0$. The anomalous magnetic frequency shift of the pantograph mode is thus proportional to the dimer spin correlator. This also follows from the calculation of the corresponding spin-phonon coupling constant [33] that assumes a particular power-law u dependence of J [34].

Optical phonons and magnetic excitations have been extensively studied in $SrCu_2(BO_3)_2$ using Raman spectroscopy at ambient pressure [33,35–37]. In the present work we perform similar measurements in a 1-mm-culet diamond-anvil cell at pressures up to 34 kbar using a Trivista 557 triple-grating spectrometer and a liquid-nitrogen-cooled CCD detector. The data were collected in a backscattering geometry using a focusing microscope. The incident laser wavelength was 532 nm. The cell environment was a He-flow cryostat with a base temperature of 2.5 K. The pressure transmitting medium was argon. The pressure was determined *in situ* from the shift of the ruby R_1 fluorescence line [38,39]. The temperature dependence of the effect, which becomes particularly important above 50 K, was explicitly corrected for Ref. [40]. The pressure changes below 40 K are marginal [Fig. 2(a)]. Most of the pressure change due to thermal expansion and solidification of argon occurs between room temperature and 40 K [Fig. 2(b)].

All pressure values quoted below correspond to base temperature readings. All experiments were performed on a $\sim 0.2 \times 0.1 \times 0.05$ mm^3 single-crystal sample extracted from cleaving a crystal grown using the floating-zone technique. The incident light was perpendicular to the ab cleavage plane (see the inset in Fig. 3). Unless otherwise noted, all spectra shown were measured in the $\bar{c}(a'b')c$ scattering geometry.
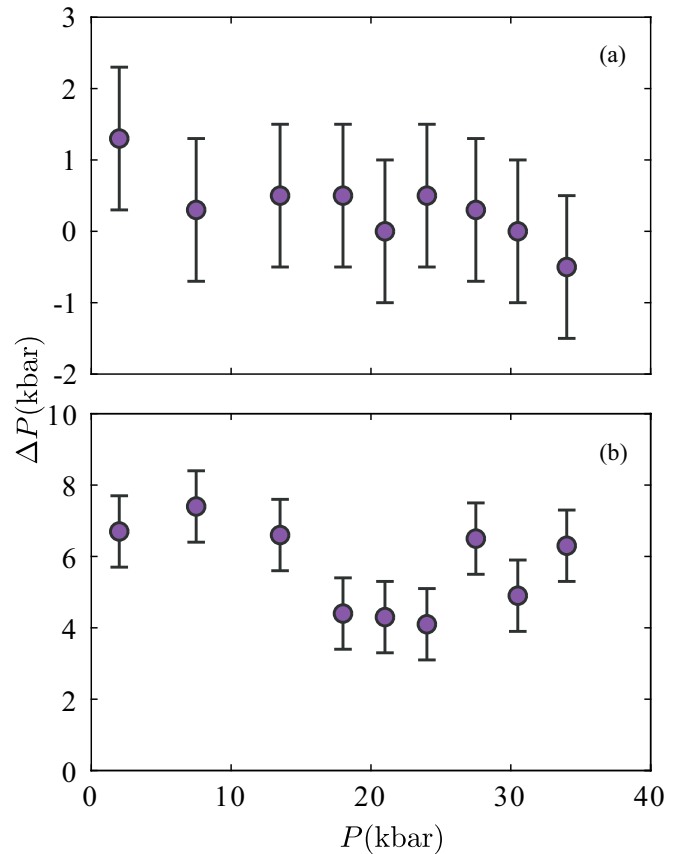

FIG. 2. (a) Measured pressure changes between 40 K and base temperature. (b) Measured pressure changes between room temperature and 40 K.

An independently measured background from the pressure transmitting medium was subtracted from all spectra.

Optical measurements on $SrCu_2(BO_3)_2$ are extremely challenging due to the narrow band gap of the material, which leads to high absorption [37]. The biggest problem is unwanted heating of the sample by the incident laser beam. To suppress this effect, the data were collected at very low power, as low as 0.05 mW at the lowest temperatures. As a result, typical counting times were as much as 72 h. In all cases it was verified that further reducing the power had no effect on the resulting spectra. A typical low-energy Raman spectrum collected in $SrCu_2(BO_3)_2$ at a pressure of $P = 2$ kbar and $T = 2.6$ K is shown in Fig. 3(a). The observed frequencies appear fully consistent with previous measurements at ambient pressure [36]. The three visible lowest-energy excitations are magnetic in origin: two triplets and one singlet. All remaining peaks are phonons. The peak widths are in all cases below 1 cm^{-1} and correspond to the expected instrumental resolution. Since data for the entire spectrum are accumulated concurrently, this confirms that the temporal drift of the spectrometer alignment during the long data collection period is a nonissue.

The pantograph mode is the peak at around 198 cm^{-1}. It was identified by a density functional theory (DFT) *ab initio* calculation with the QUANTUM ESPRESSO software package [41], using the SSSP Accuracy (version 1.1) pseudopotential
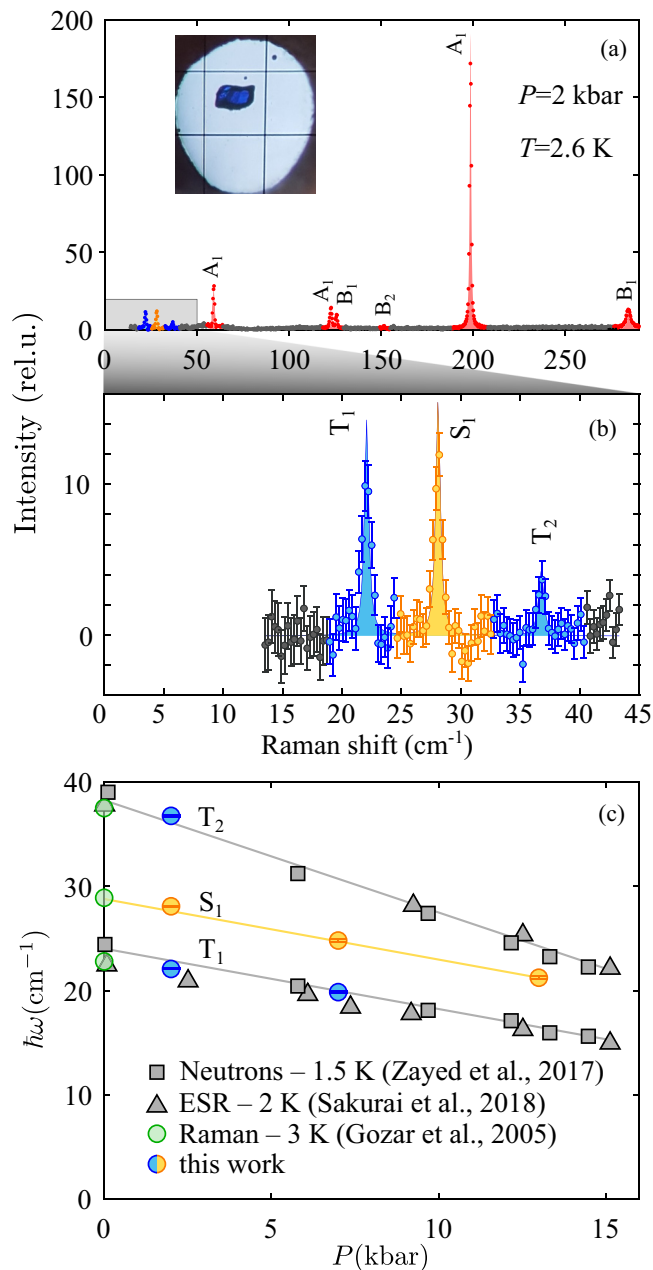
FIG. 3. (a) Raman data at $T \approx 2.6$ K and 2 kbar in $\bar{c}(a'b')c$ polarization measured with a $\lambda = 532$ nm laser. Symmetries of phonons are assigned as in Ref. [36]. Inset: Picture of the single-crystal sample inside the pressure cell along with two ruby spheres used for pressure calibration. (b) Blowup of the low-energy portion of (a). Triplets T_1 and T_2 and singlet S_1 are assigned according to Ref. [36]. (c) Comparison of excitation energies of singlet and triplet excitations to published results [23,27,36].

library [42–48]. The kinetic energy cutoff was 120 Ry and the charge density cutoff 600 Ry. Brillouin zone integration was performed using a $4 \times 4 \times 4$ k-point grid. For better convergence a Marzari-Vanderbilt cold smearing of 0.01 Ry was applied.

In order to validate the experimental methodology we first checked the behavior of the three *magnetic* excitations. With
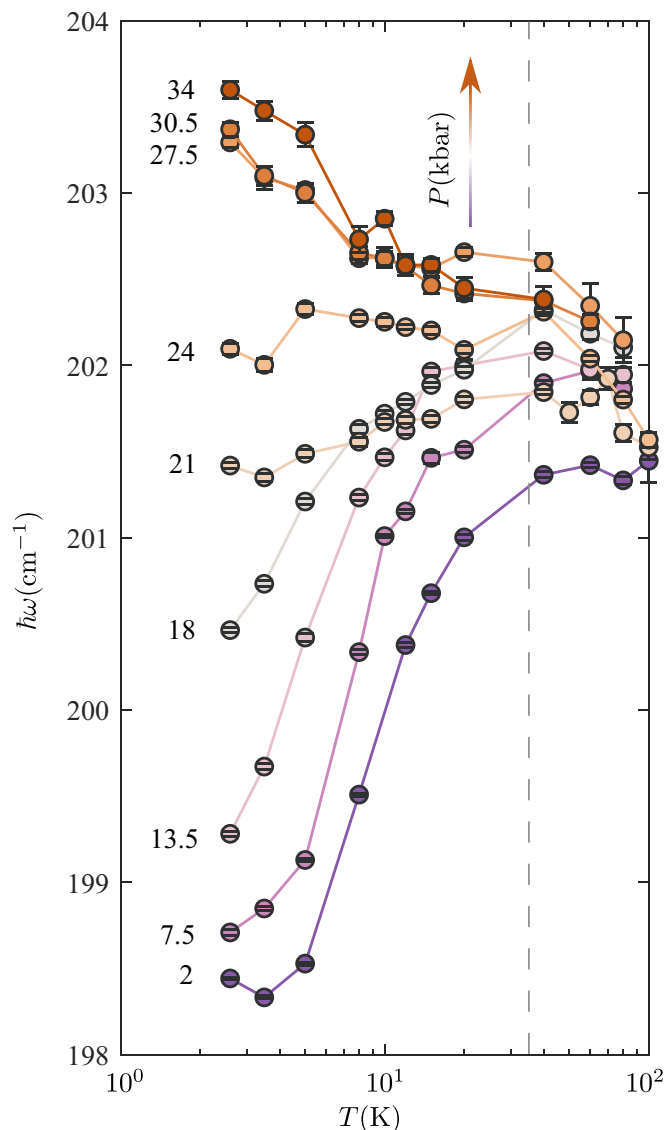

FIG. 4. Measured temperature dependence of the pantograph mode frequency in $SrCu_2(BO_3)_2$ at different pressures. Note the logarithmic temperature scale. The dashed line is the temperature corresponding to the spin gap energy at ambient pressure.

increasing pressure all three peaks shift to lower energies and progressively weaken. Their measured frequencies are plotted in colored circles in Fig. 3(c). At higher pressures they become undetectably weak or shift outside our measurement window (T_1). The observed softening of the triplet modes is fully consistent with previous electron spin resonance (ESR) [27] and inelastic neutron scattering [23] studies, shown as triangles and squares in the figure. The softening of the singlet mode is a different result, since neither ESR nor neutrons are sensitive to singlet-singlet transitions.

The central result of this Rapid Communication is the observation of an anomalous temperature dependence of the pantograph mode, as visualized in Fig. 4. Note the logarithmic temperature scale. At all pressures, the pantograph mode undergoes at most a modest hardening upon cooling down to 40 K. This behavior is due to the usual anharmonicities of
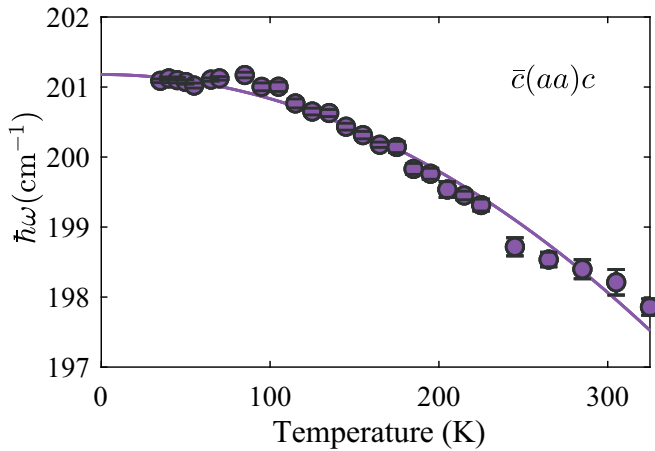
FIG. 5. Measured temperature dependence of the pantograph mode in SrCu$_2$(BO$_3$)$_2$ at ambient pressure (symbols) and fit assuming anharmonic multiphonon coupling (solid line).

lattice vibrations and the temperature dependence of pressure in the loaded cell at higher temperatures.

At temperatures below 40 K the anharmonic thermal frequency shift of the pantograph mode is negligible. In order to establish this, we measured the temperature dependence of the pantograph mode frequency between 35 K and room temperature at ambient pressure. The result is visualized in Fig. 5 (symbols). These data were analyzed using the well-known predictions for anharmonic multiphonon coupling [Eq. (3.9) in Ref. [49]]. An excellent fit is obtained using empirical parameters $\omega_0 = 201.2$ cm^{-1}, $C = 0$, and $D = -2.7(1) \times 10^{-3}$ cm^{-1} (solid line in Fig. 5). Extrapolating this curve to below 40 K yields an estimate of the anharmonic shift in the low-temperature range, $\delta\omega \lesssim 0.1$ cm^{-1}. This is considerably smaller than the observed anomalous magnetic frequency shift and can be safely disregarded.

Below this point the mode suddenly becomes strongly T dependent. At low applied pressures it *softens* upon cooling to the base temperature by as much as 1.5%. At the highest pressures the effect is reversed: In the same low-temperature interval the excitation hardens by as much as 0.5%. Also revealing is the pressure dependence at different temperatures shown in Fig. 6(a). For $T \gtrsim 40$ K the pressure dependencies are almost T independent. They all show a monotonous hardening with a small but reproducible dip at about 20 kbar. At lower temperatures the situation changes drastically, the frequency showing a steep, almost steplike, increase.

As established above, at temperatures below 40 K anharmonic effects extrapolated from measurements above 35 K are entirely negligible. The only remaining relevant energy scale is the magnetic one. We conclude that the anomalous temperature dependence of the pantograph mode is due to magnetoelastic coupling. The corresponding relative frequency shift between 40 and 2.6 K is plotted against pressure in Fig. 6(b) (left axis). As mentioned above, the cell pressure is practically constant in this temperature range. The shift remains flat up to about $P_1 \sim 15$ kbar and then steadily increases up to the highest attainable pressures, switching sign at about $P_2 \sim 22$ kbar.

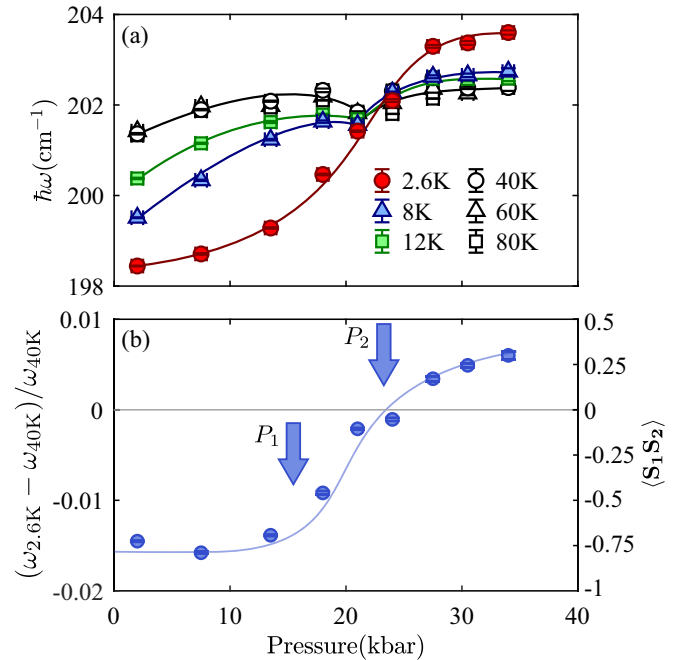

FIG. 6. (a) Measured pressure dependence of the pantograph mode frequency in SrCu$_2$(BO$_3$)$_2$ at several different temperatures (symbols). The lines are guides for the eye. (b) Pressure dependence of the low-temperature frequency shift of the pantograph mode. P_1 indicates the beginning of the destruction of dimer correlations and P_2 denotes the sign switching of dimer correlations. The solid line is a guide to the eye.

As shown by ESR experiments [27], J' decreases by only about 12% from 0 to 15 kbar. This allows us to assume that the second derivative in Eq. (1) is also *only weakly pressure dependent* to some approximation. The lack of any pressure dependence for $P \lesssim P_1$ in Fig. 6(b) confirms this. Here, the system is clearly in the dimer phase [23]. In this regime the exact result is $\langle \mathbf{S}_1 \mathbf{S}_2 \rangle \equiv -\frac{3}{4}$ regardless of J'/J [3], and the measured constant frequency shift implies a constant $\partial^2 J'/\partial u^2$. Assuming the trend continues at higher pressures, to within a scale factor, Fig. 6(b) represents the pressure dependence of $\langle \mathbf{S}_1 \mathbf{S}_2 \rangle$. The exact value for the dimer phase provides a calibration for the entire plot [Fig. 6(b), right axis]. At P_2 the relative alignment of nearest-neighbor spins *switches sign and becomes predominantly ferromagnetic*.

That AF dimers are replaced by a completely different spin correlation pattern already at rather low pressures is significant. The only other indication of that are the rather tenuous 22-kbar structure factor data from the neutron study of Ref. [23]. The transformation that we observe starts already at about 15 kbar. It can only be driven by a subtle change in the J'/J ratio, as assumed in most theoretical studies [2–20]. It takes place long before the exchange constants themselves can be expected to switch sign [27]. It also seems not to be associated with any structural transition, of which we do not observe any obvious signs such as splitting of phonon lines or the appearance of different modes.

According to a recent calorimetric study [24], there is a distinct thermodynamic phase that emerges below $T_c \sim 2$ K just about P_1. The authors suggest that it may be a plaquette

state. The sign switching reported here is consistent with that interpretation. While in the dimer phase the spin correlations are AF, in the plaquette state they at least partially switch to FM and may evolve continuously [17,20]. Unfortunately, the lowest attainable temperature in our experiments is slightly above T_c. The observed behavior can be interpreted as a change in the character of dominant *short-range* spin correlations, which are just about to order in another plaquette configuration upon further cooling. According to Ref. [24], Néel magnetic order sets in above approximately P_2. Here, even stronger FM correlations are predicted [17], and indeed observed in our measurements.

In summary, our measurements of the pantograph mode in $SrCu_2(BO_3)_2$ provide an indirect but precise measurement of a pressure-induced sign switching of nearest-neighbor dimer spin correlations. We hope that a quantitative comparison with theoretical studies will become possible in the future.

[1] B. S. Shastry and B. Sutherland, Exact ground state of a quantum mechanical antiferromagnet, Physica B+C **108**, 1069 (1981).

[2] M. Albrecht and F. Mila, First-order transition between magnetic order and valence bond order in a 2D frustrated Heisenberg model, Europhys. Lett. **34**, 145 (1996).

[3] S. Miyahara and K. Ueda, Exact Dimer Ground State of the Two Dimensional Heisenberg Spin System $SrCu_2(BO_3)_2$, Phys. Rev. Lett. **82**, 3701 (1999).

[4] Zeng Weihong, C. J. Hamer, and J. Oitmaa, Series expansions for a Heisenberg antiferromagnetic model for $SrCu_2(BO_3)_2$, Phys. Rev. B **60**, 6608 (1999).

[5] A. Koga and N. Kawakami, Quantum Phase Transitions in the Shastry-Sutherland Model for $SrCu_2(BO_3)_2$, Phys. Rev. Lett. **84**, 4461 (2000).

[6] E. Müller-Hartmann, R. R. P. Singh, C. Knetter, and G. S. Uhrig, Exact Demonstration of Magnetization Plateaus and First-Order Dimer-Néel Phase Transitions in a Modified Shastry-Sutherland Model for $SrCu_2(BO_3)_2$, Phys. Rev. Lett. **84**, 1808 (2000).

[7] Y. Takushima, A. Koga, and N. Kawakami, Competing spin-gap phases in a frustrated quantum spin system in two dimensions, J. Phys. Soc. Jpn. **70**, 1369 (2001).

[8] D. Carpentier and L. Balents, Field theory for generalized Shastry-Sutherland models, Phys. Rev. B **65**, 024427 (2001).

[9] C. H. Chung, J. B. Marston, and S. Sachdev, Quantum phases of the Shastry-Sutherland antiferromagnet: Application to $SrCu_2(BO_3)_2$, Phys. Rev. B **64**, 134407 (2001).

[10] W. Zheng, J. Oitmaa, and C. J. Hamer, Phase diagram of the Shastry-Sutherland antiferromagnet, Phys. Rev. B **65**, 014408 (2001).

[11] A. Läuchli, S. Wessel, and M. Sigrist, Phase diagram of the quadrumerized Shastry-Sutherland model, Phys. Rev. B **66**, 014401 (2002).

[12] M. Al Hajj and J.-P. Malrieu, Phase transitions in the Shastry-Sutherland lattice, Phys. Rev. B **72**, 094436 (2005).

[13] R. Darradi, J. Richter, and D. J. J. Farnell, Coupled cluster treatment of the Shastry-Sutherland antiferromagnet, Phys. Rev. B **72**, 104425 (2005).

[14] A. Isacsson and O. F. Syljuåsen, Variational treatment of the Shastry-Sutherland antiferromagnet using projected entangled pair states, Phys. Rev. E **74**, 026701 (2006).

[15] S. Moukouri, Plaquette ground state of the Shastry-Sutherland model: Density-matrix renormalization-group calculations, Phys. Rev. B **78**, 132405 (2008).

[16] M. Moliner, I. Rousochatzakis, and F. Mila, Emergence of one-dimensional physics from the distorted Shastry-Sutherland lattice, Phys. Rev. B **83**, 140414(R) (2011).

[17] P. Corboz and F. Mila, Tensor network study of the Shastry-Sutherland model in zero magnetic field, Phys. Rev. B **87**, 115144 (2013).

[18] D. C. Ronquillo and M. R. Peterson, Identifying topological order in the Shastry-Sutherland model via entanglement entropy, Phys. Rev. B **90**, 201108(R) (2014).

[19] Z. Wang and C. D. Batista, Dynamics and Instabilities of the Shastry-Sutherland Model, Phys. Rev. Lett. **120**, 247201 (2018).

[20] C. Boos, S. P. G. Crone, I. A. Niesen, P. Corboz, K. P. Schmidt, and F. Mila, Competition between intermediate plaquette phases in $SrCu_2(BO_3)_2$ under pressure, Phys. Rev. B **100**, 140413 (2019).

[21] H. Kageyama, K. Yoshimura, R. Stern, N. V. Mushnikov, K. Onizuka, M. Kato, K. Kosuge, C. P. Slichter, T. Goto, and Y. Ueda, Exact Dimer Ground State and Quantized Magnetization Plateaus in the Two-Dimensional Spin System $SrCu_2(BO_3)_2$, Phys. Rev. Lett. **82**, 3168 (1999).

[22] C. Knetter and G. S. Uhrig, Dynamic Structure Factor of the Two-Dimensional Shastry-Sutherland Model, Phys. Rev. Lett. **92**, 027204 (2004).

[23] M. E. Zayed, Ch. Rüegg, A. M. Läuchli, C. Panagopoulos, S. S. Saxena, M. Ellerby, D. F. McMorrow, Th. Strässle, S. Klotz, G. Hamel *et al.*, 4-spin plaquette singlet state in the Shastry-Sutherland compound $SrCu_2(BO_3)_2$, Nat. Phys. **13**, 962 (2017).

[24] J. Guo, G. Sun, B. Zhao, L. Wang, W. Hong, V. A. Sidorov, N. Ma, Q. Wu, S. Li, Z. Y. Meng, A. W. Sandvik, and L. Sun, Quantum phases of $Sr_2Cu_2(BO_3)_2$ from high-pressure thermodynamics, arXiv:1904.09927.

[25] S. Haravifard, A. Banerjee, J. C. Lang, G. Srajer, D. M. Silevitch, B. D. Gaulin, H. A. Dabkowska, and T. F. Rosenbaum, Continuous and discontinuous quantum phase transitions in a model two-dimensional magnet, Proc. Natl. Acad. Sci. USA **109**, 2286 (2012).

[26] T. Waki, K. Arai, M. Takigawa, Y. Saiga, Y. Uwatoko, H. Kageyama, and Y. Ueda, A novel ordered phase in $SrCu_2(BO_3)_2$ under high pressure, J. Phys. Soc. Jpn. **76**, 073710 (2007).

[27] T. Sakurai, Y. Hirao, K. Hijii, S. Okubo, H. Ohta, Y. Uwatoko, K. Kudo, and Y. Koike, Direct observation of the quantum phase transition of $SrCu_2(BO_3)_2$ by high-pressure and terahertz electron spin resonance, J. Phys. Soc. Jpn. **87**, 033701 (2018).

[28] C. Raas, U. Löw, G. S. Uhrig, and R. W. Kühne, Spin-phonon chains with bond coupling, Phys. Rev. B **65**, 144438 (2002).

[29] K.-Y. Choi, A. Oosawa, H. Tanaka, and P. Lemmens, Interplay of triplets and lattice degrees of freedom in the coupled spin dimer system $KCuCl_3$, Phys. Rev. B **72**, 024451 (2005).

[30] S. Bettler, G. Simutis, G. Perren, D. Blosser, S. Gvasaliya, and A. Zheludev, High-pressure Raman study of the quantum magnet $(C_4H_{12}N_2)Cu_2Cl_6$, Phys. Rev. B **96**, 174431 (2017).

[31] G. Radtke, A. Saúl, H. A. Dabkowska, M. B. Salamon, and M. Jaime, Magnetic nanopantograph in the $SrCu_2(BO_3)_2$ Shastry-Sutherland lattice, Proc. Natl. Acad. Sci. USA **112**, 1971 (2015).

[32] C. Vecchini, O. Adamopoulos, L. C. Chapon, A. Lappas, H. Kageyama, Y. Ueda, and A. Zorko, Structural distortions in the spin-gap regime of the quantum antiferromagnet $SrCu_2(BO_3)_2$, J. Solid State Chem. **182**, 3275 (2009).

[33] K.-Y. Choi, Yu. G. Pashkevich, K. V. Lamonova, H. Kageyama, Y. Ueda, and P. Lemmens, Strong anharmonicity and spin-phonon coupling in the quasi-two-dimensional quantum spin system $Sr_{1-x}Ba_xCu_2(BO_3)_2$, Phys. Rev. B **68**, 104418 (2003).

[34] S. Miyahara and K. Ueda, Theory of the orthogonal dimer Heisenberg spin model for $SrCu_2(BO_3)_2$, J. Phys.: Condens. Matter **15**, R327 (2003).

[35] P. Lemmens, M. Grove, M. Fischer, G. Güntherodt, V. N. Kotov, H. Kageyama, K. Onizuka, and Y. Ueda, Collective Singlet Excitations and Evolution of Raman Spectral Weights in the 2D Spin Dimer Compound $SrCu_2(BO_3)_2$, Phys. Rev. Lett. **85**, 2605 (2000).

[36] A. Gozar, B. S. Dennis, H. Kageyama, and G. Blumberg, Symmetry and light coupling to phononic and collective magnetic excitations in $SrCu_2(BO_3)_2$, Phys. Rev. B **72**, 064405 (2005).

[37] C. C. Homes, S. V. Dordevic, A. Gozar, G. Blumberg, T. Rõõm, D. Hüvonen, U. Nagel, A. D. LaForge, D. N. Basov, and H. Kageyama, Infrared spectra of the low-dimensional quantum magnet $SrCu_2(BO_3)_2$: Measurements and *ab initio* calculations, Phys. Rev. B **79**, 125101 (2009).

[38] Y. Feng, R. Jaramillo, J. Wang, Y. Ren, and T. F. Rosenbaum, Invited article: High-pressure techniques for condensed matter physics at low temperature, Rev. Sci. Instrum. **81**, 041301 (2010).

[39] C.-S. Zha, H.-k. Mao, and R. J. Hemley, Elasticity of MgO and a primary pressure scale to 55 GPa, Proc. Natl. Acad. Sci. USA **97**, 13494 (2000).

[40] D. D Ragan, R. Gustavsen, and D. Schiferl, Calibration of the ruby R_1 and R_2 fluorescence shifts as a function of temperature from 0 to 600 K, J. Appl. Phys. **72**, 5539 (1992).

[41] P. Giannozzi, S. Baroni, N. Bonini, M. Calandra, R. Car, C. Cavazzoni, D. Ceresoli, G. L. Chiarotti, M. Cococcioni, I. Dabo, A. D. Corso, S. de Gironcoli, S. Fabris, G. Fratesi, R. Gebauer, U. Gerstmann, C. Gougoussis, A. Kokalj, M. Lazzeri, L. Martin-Samos *et al.*, Quantum Espresso: A modular and open-source software project for quantum simulations of materials, J. Phys.: Condens. Matter **21**, 395502 (2009).

[42] G. Prandini, A. Marrazzo, I. E. Castelli, N. Mounet, and N. Marzari, Precision and efficiency in solid-state pseudopotential calculations, npj Comput. Mater. **4**, 72 (2018).

[43] K. Lejaeghere, G. Bihlmayer, T. Björkman, P. Blaha, S. Blügel, V. Blum, D. Caliste, I. E. Castelli, S. J. Clark, A. Dal Corso, S. de Gironcoli, T. Deutsch, J. K. Dewhurst, I. Di Marco, C. Draxl, M. Dułak, O. Eriksson, J. A. Flores-Livas, K. F. Garrity, L. Genovese *et al.*, Reproducibility in density functional theory calculations of solids, Science **351**, aad3000 (2016).

[44] D. R. Hamann, Optimized norm-conserving Vanderbilt pseudopotentials, Phys. Rev. B **88**, 085117 (2013).

[45] M. Schlipf and F. Gygi, Optimization algorithm for the generation of ONCV pseudopotentials, Comput. Phys. Commun. **196**, 36 (2015).

[46] G. Prandini, A. Marrazzo, I. E. Castelli, N. Mounet, and N. Marzari, A standard solid state pseudopotentials (SSSP) library optimized for precision and efficiency (version 1.1, data download), doi:10.24435/materialscloud:2018.0001/v3 (2018).

[47] K. F. Garrity, J. W. Bennett, K. M. Rabe, and D. Vanderbilt, Pseudopotentials for high-throughput DFT calculations, Comput. Mater. Sci. **81**, 446 (2014).

[48] A. D. Corso, Pseudopotentials periodic table: From H to Pu, Comput. Mater. Sci. **95**, 337 (2014).

[49] M. Balkanski, R. F. Wallis, and E. Haro, Anharmonic effects in light scattering due to optical phonons in silicon, Phys. Rev. B **28**, 1928 (1983).